Mapping Land Subsidence in Ahmedabad City, India: Interpreting InSAR-Derived Land Subsidence with Auxiliary Data

Ankur Pandit[1], Nishtha Ahuja[2], Suryakant Sawant[3], Jayantrao Mohite[4], Srinivasu Pappula[5]*

[1] Tata Consultancy Services, Research and Innovation, Super Corridor Road, Indore, Madhya Pradesh, India
[2] Dhirubhai Ambani Institute of Information and Communication Technology, Gandhinagar, Gujarat, India
[3] Tata Consultancy Services, Research and Innovation, TRDDC, Pune, Maharashtra, India
[4] Tata Consultancy Services, Research and Innovation, Pokharan Road, Thane West, Maharashtra, India
[5] Tata Consultancy Services, Research and Innovation, Hyderabad, Telangana, India
*Corresponding Author – ankur.pandit@tcs.com

KEY WORDS: Land subsidence, InSAR, SBAS, Sentinel-1, Ahmedabad

ABSTRACT:

In this study, we mapped land subsidence in the Ahmedabad urban region using the SBAS InSAR technique between 2020 and 2023 (approximately 3.5 years). A distinct pattern of average line of sight (LOS) land subsidence was observed at two key locations within the city: the Southwest and Southeast regions of Ahmedabad. The average LOS velocity in these areas ranged from -1.5 cm/year to -3.0 cm/year in the Southwest and -2 cm/year to -3.5 cm/year in the Southeast. Negative LOS velocities represent areas experiencing subsidence. Data from the Central Ground Water Board (CGWB) revealed that groundwater levels in the Southwest region dropped significantly from around 11 meters in mid-2005 to less than 2 meters by 2019. Similarly, in the Southeast, groundwater levels fell from approximately 42 meters in 2005 to around 28 meters in 2019. The observed land subsidence was strongly correlated with localized groundwater depletion. Additionally, groundwater data from multiple wells across the Ahmedabad district were analyzed over several years. In contrast to localized depletion, a substantial number of wells at the district level showed an increase in groundwater levels from 2014 to 2022, compared to the decadal average, suggesting an overall positive trend in groundwater availability. This indicates that the subsidence is likely due to localized over-extraction of groundwater and hydrogeological factors specific to these areas, which differ from broader regional trends.

1. INTRODUCTION

Land subsidence refers to the gradual sinking or settling of the Earth's surface, often occurring due to natural or human-induced factors or as a combination of both natural and anthropogenic processes. This phenomenon can have significant environmental, economic, and social implications, particularly in urban and agricultural areas. Studies have reported land subsidence in various parts of the world, with major causes including groundwater extraction (e.g., Cigna and Tapete 2021; Ghorbani et al. 2022; Kumar et al. 2022), urbanization (e.g., Dong et al. 2014; Chen et al. 2018; Cigna and Tapete 2022), oil and gas extraction (e.g., Fatholahi et al. 2018; Zakaria et al. 2023), and earthquakes (e.g., Albano et al. 2014; Hejmanowski et al. 2019). Many studies highlighted that the excessive groundwater extraction is one of the most significant human-induced causes of land subsidence. Land subsidence due to groundwater extraction happens when water is pumped out of underground aquifers faster than it can be naturally replenished. When groundwater is excessively withdrawn, the resulting decrease in pore-fluid pressure increases the stress on the soil structure. This increased stress can cause the soil to compress, leading to irreversible compaction of the aquifer and potential land subsidence (Sneed and Brandt 2007). This process is accelerated in areas with extensive groundwater use for agriculture, urbanization, and industry, leading to infrastructure damage, reduced water storage capacity, and increased flood susceptibility.

In India, out of the 6,553 assessment units across the country, 736 units (11.23%) have been classified as 'Over-exploited,' meaning groundwater extraction surpasses the annual replenishment rate. In 199 units (3.04%), groundwater extraction is between 90-100%, classifying them as 'Critical.' Additionally, 698 units (10.65%) are deemed 'Semi-critical,' where groundwater extraction ranges from 70% to 90% (Central Ground Water Board 2023). Due to the widespread availability of groundwater, it is readily accessible and constitutes the largest portion of the country's agricultural and drinking water supply . The irrigation sector utilizes 89% of extracted groundwater, making it the primary consumer (Annual Report 2013-14, Ministry of Water Resources). Groundwater for domestic purposes accounts for 9% of total extraction, while industrial use accounts for 2%. Additionally, groundwater satisfies 50% of urban water needs and 85% of rural domestic water needs (Suhag 2016). Ground water depletion due to overexploitation caused land subsidence in urban region e.g. Delhi (Garg et al. 2022), Ludhiana (Shankar et al. 2024), Gandhinagar (Choudhury et al. 2018), Kolkata (Sahu and Sikdar 2011), Chandigarh (Kadiyan et al. 2021) of India.

In the past, studies have utilized Global Positioning System (GPS) measurements to observe land subsidence (e.g. Ikehara 1994; Sharif et al. 1997; Abidin et al. 2008). GPS surveys typically consist of point measurements or a network of stationary stations, which may not uniformly capture subsidence across extensive or diverse landscapes. Achieving comprehensive spatial coverage can therefore be difficult (Abidin et al. 2008). Moreover, continuous monitoring of subsidence necessitates frequent GPS surveys to monitor changes over time. However, conducting these surveys frequently can be expensive and time-consuming, thus limiting the frequency of data collection. Additionally, the costs associated with GPS surveys, including equipment, personnel, and operational expenses, can be substantial, especially for long-term monitoring efforts spanning large study areas.

Alternatively, interferometric synthetic aperture radar (InSAR) (Gabriel et al. 1989) techniques have be used worldwide for land subsidence monitoring (e.g. Dehghani et al. 2009; Aobpaet et al. 2013; Chaussard et al. 2014; current study). InSAR is a powerful remote sensing technique used for monitoring land subsidence with high precision and spatial coverage (Ferretti et al. 2015).

Fundamentally, InSAR compares radar images acquired at different time periods over the same area. Subsidence causes changes in the distance travelled by radar waves between the satellite and the ground surface over time. These changes alter the interference patterns in the radar images, allowing precise measurement of subsidence rates. (Chen et al. 2000). Currently, Sentinel-1 is equipped with InSAR capabilities, allowing for precise measurements of ground deformation. Sentinel-1 is a radar imaging satellite mission operated by the European Space Agency (ESA) as part of the Copernicus program, specifically designed for Earth observation (Torres et al. 2012). Sentinel-1 carries a SAR instrument that operates in the C-band (5.405 GHz) with a repeat cycle of 12 days and acquire data in Interferometric Wide Swath (IW) mode for wide-area coverage with a swath width of up to 250 km under all weather conditions and day or night. Sentinel-1 data is freely and openly accessible to users worldwide.

Ahmedabad, a major city in the western state of Gujarat, faces significant challenges related to groundwater depletion, as reported by the Central Ground Water Board (CGWB) (https://cgwb.gov.in/). This study focuses on examining the impact of groundwater extraction on surface deformation in the city's urban area and explores other possible contributing factors, such as urbanization and irrigation that may be causing land subsidence. To map land subsidence in Ahmedabad, time-series Sentinel-1 InSAR data from 2020 to 2023 were used.

2. MATERIALS AND METHODS

2.1 Study Area

Ahmedabad (Figure 1) is a major city in Gujrat, India, with a population of almost 74 lakhs (7.4 Million). The city is located on the banks of the River Sabarmati which is the main river passing through the central part of the urban area. The Sabarmati River divides Ahmedabad into two large regions, the eastern and the western region with a historic center located at the eastern bank of the river (Lehner et al. 2016). Intense farming methods combined with heavy water extraction for crops result in the river becoming completely dry once it reaches the boundaries of Ahmedabad city (Gupte et al. 2009). A LANDSAT satellite-based study conducted by Chaturvedi et al. 2022 highlighted that in between year 1990-2019, the total built-up area of Ahmedabad was expanded by 130%, 132 km^2 in 1990 to 305 km^2 in 2019. Same study (Chaturvedi et al. 2022) also predicts a 25% and 19% increase in Ahmedabad’s total urban area and population by 2030.

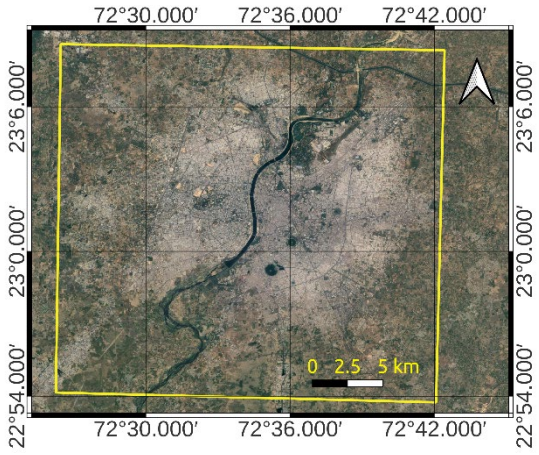

Figure 1: Ahmedabad urban region (in yellow bounding box)

2.2 Data used

In this research, a dataset of 110 single-look complex (SLC) images of C-band Sentinel-1A SAR (5.405 GHz central frequency *f*, and 5.547 cm wavelength λ) acquired in descending orbit and in Interferometric Wide (IW) imaging mode was used. Sentinel-1A satellite images from Apr 2020 to Dec 2023 in a time interval of 12 days were used. The employed acquisition mode was the Interferometric Wide (IW) swath, which is based on the Terrain Observation with Progressive Scans (TOPS) ScanSAR mode (De Zan and Guarnieri, 2006). IW creates images with a 250 km swath at 5×20 m spatial resolution. We selected interferometric pairs with small perpendicular baselines and temporal base-lines of 200 m and 60 days, respectively.

For additional analysis, the yearly rainfall (in mm) and % departure of Ahmedabad district (Figure 2) from year 2014 to 2022 was obtained from CGWB (source: https://www.cgwb.gov.in/). The data from the CGWB reveals notable fluctuations in annual rainfall, with significant deficits in 2016, 2018, 2021, and 2022, and surpluses in 2017 and 2019. The years 2014 and 2020 have departures closer to zero, implying near-average rainfall. This variability suggests that rainfall patterns have been irregular, with some years experiencing much lower or higher than average precipitation.

Also, we have collected yearly time-series area and production data for rice and wheat crop for the Ahmedabad region (data source- https://dag.gujarat.gov.in) (Figure 3a). Additionally, yearly time-series area (Figure 3b) and production (Figure 3c) of wheat crop (cultivated during post monsoon Rabi season- Oct to Mar) for the Ahmedabad region under irrigated and unirrigated condition were also collected.

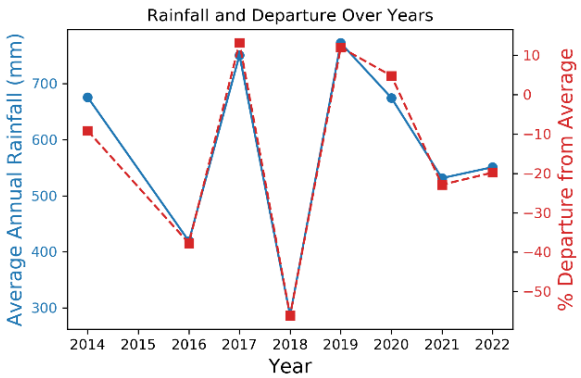

Figure 2: Yearly rainfall (in mm) and % departure of Ahmedabad district (data source: https://www.cgwb.gov.in/)

2.3 Method

The complete data processing was performed on two different platforms - (a) Alaska Satellite Facility (ASF) Hybrid Pluggable Processing Pipeline (Hyp3) on-demand InSAR processing platform (Hogenson et al. 2016) and (b) OpenSARLab (Hogenson et al. 2021). Detailed flowchart of complete workflow is mentioned in Figure 4. Figure 5 illustrated SBAS connections with temporal and perpendicular baselines of Sentinel-1A images.

This contribution has been peer-reviewed. The double-blind peer-review was conducted on the basis of the full paper.
https://doi.org/10.5194/isprs-annals-X-G-2025-613-2025 | © Author(s) 2025. CC BY 4.0 License.

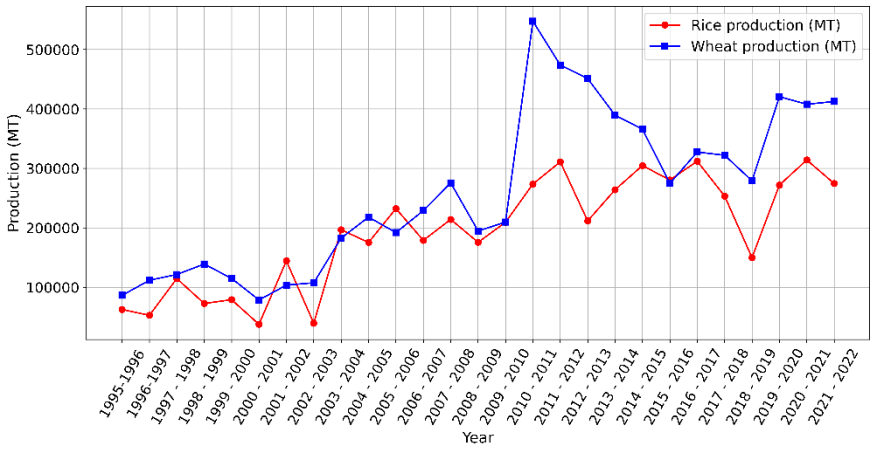

(a)

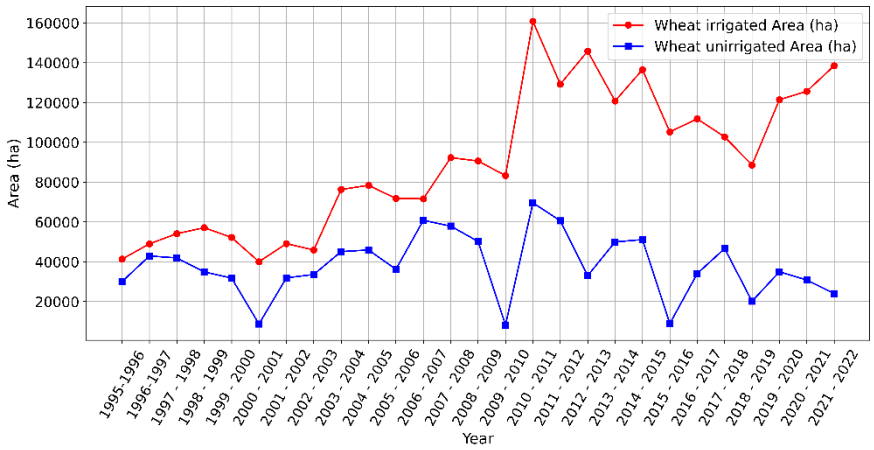

(b)

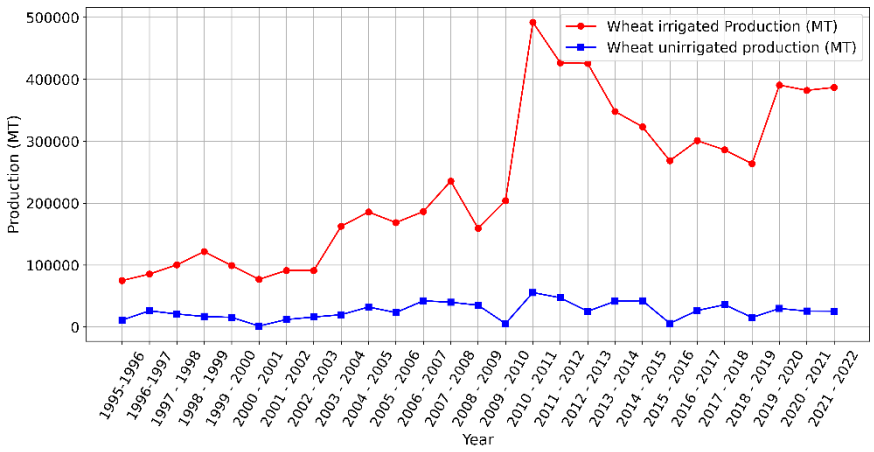

(c)

Figure 3: (a) Time-series rice and wheat crop production, Time-series (b) area and (c) production of wheat crop under irrigated and unirrigated condition

Firstly, total 498 unwrapped differential interferograms were generated based on the 110 Sentinel-1 SLC data using Hyp3 platform. The Hyp3 InSAR data processing works based on GAMMA SAR Software (Wegnüller et al. 2016) and provides multiple options setting while submitting jobs for processing. The GAMMA workflow include: pre-processing steps, interferogram preparation, and product creation. Initially, pre-processing steps prepare the SAR images to be used in interferometry. This include image selection, ingest (including calibration), creation of a suitable Digital Elevation Model (DEM), and calculation of the burst overlap. Next, workflow step includes interferogram creation, co-registration and refinement. The output of this step is a wrapped interferogram. Later, wrapped interferogram was unwrapped in phase unwrapping step using Minimum Cost Flow1 (MCF) (Wegmüller et al. 2002). After the phase is unwrapped, the final steps are geocoding and product creation.

Later, SBAS-InSAR time-series processing was performed using an open-source package called Miami INsar Time-series software in PYthon (MintPy) (Yunjun et al. 2019). The Mintpy toolbox is a Python 3 program designed for analyzing time series in small baseline InSAR and produces spatio-temporal land surface deformation in radar line-of-sight (LOS) direction. It operates on a stack of differential interferograms that create a comprehensive network. In the current study, the SBAS stack were accessed from ASF HyP3 and subsetted and later, MintPy processing were performed in the OpenSARLab which is a specific service within OpenScienceLab (OSL) that caters to SAR data analysis. It provides a free, limited-use cloud-hosted JupyterHub environment. As mentioned in Karamvasis and Karathanassi 2020, Mintpy toolbox consists of three major processing steps: (a) the raw interferometric phase time series calculation; (b) the correction of the raw phase time series from error sources; and (c) the noise evaluation step that results in the exclusion of noise SAR acquisitions and the final calculation of noise-reduced displacement time series.

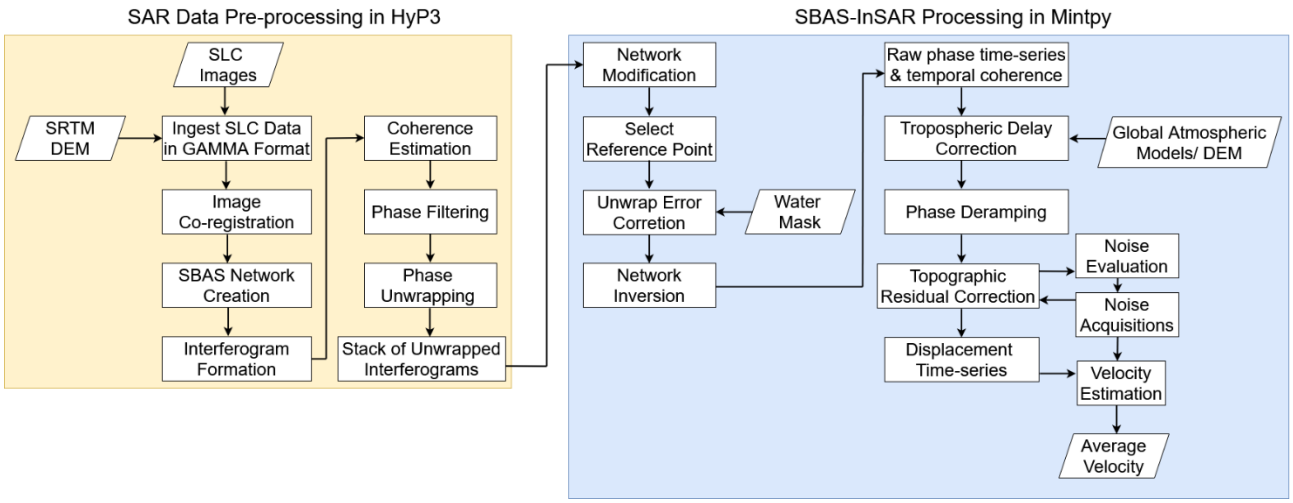

Figure 4: Overall methodology adopted in this study

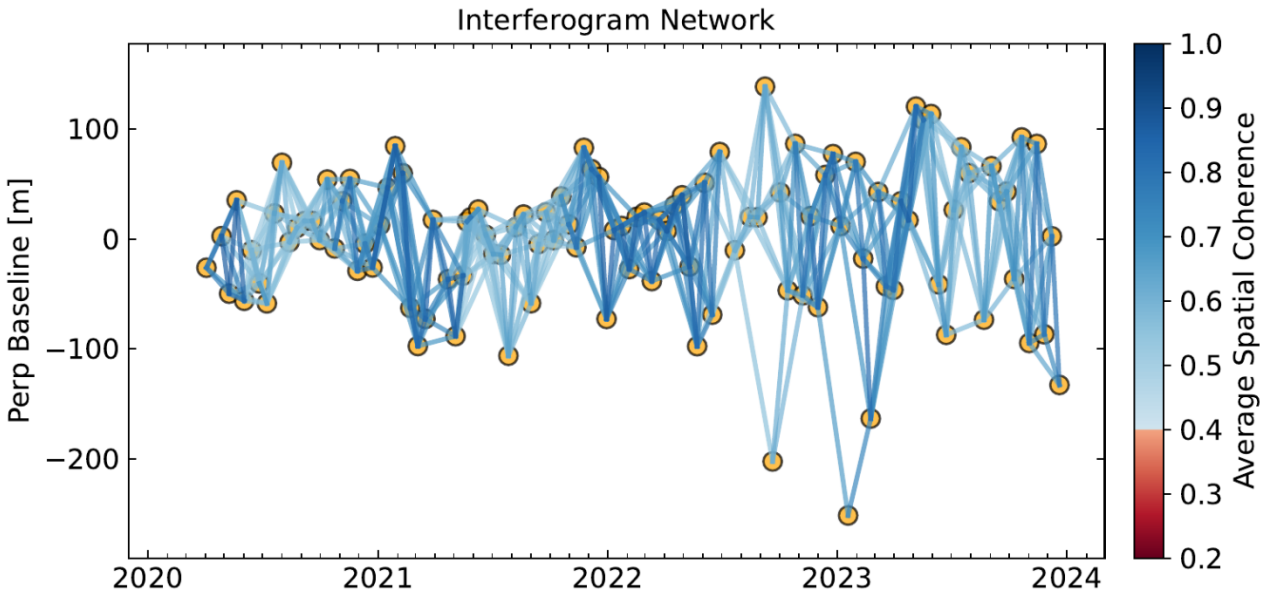

Figure 5: SBAS connections with temporal and perpendicular baselines of Sentinel-1A images

3. RESULTS AND DISCUSSION

In this study, we have processed 110 Sentinel-1A scenes in descending pass acquired over about 3.5 year period spanning from Apr 2020 to Dec 2023 to monitor subsidence in Ahmedabad urban region**.** A total of 498 SBAS connections (interferogram) were formed (Figure 5). Complete analysis was performed on ASF’s Hyp3 processing platform and OpenSARLab. This section is discussed in two separate subsections- Section 3.1 discusses mean LOS velocity measurements derived from SBAS InSAR and Section 3.2 discusses the insights derived from groundwater level data collected from various wells distributed throughout the Ahmedabad district. Section 3.3 addresses one of the key contributors to groundwater depletion, specifically its use for agricultural purposes. Other potential factors, such as population growth, urbanization, and climate change, are not covered in this study due to the absence of dense time-series datasets for limited study period.

3.1 Mean LOS velocity measurement

The study utilized the SBAS InSAR technique, an advanced form of DInSAR, to identify land subsidence in the urban Ahmedabad urban. Figure 6 displays the coherence map derived for the Ahmedabad region along with the differential interferogram. Here, the brighter regions indicate higher coherence or less noisy phase, aligning with urban features like buildings and houses that exhibit minimal temporal changes. Conversely, darker regions correspond to agricultural areas with lower coherence values (or noisy phase), attributed to vegetation's temporal variability leading to decorrelation in the interferometric phase. Therefore, a coherence threshold of 0.8 was established to isolate and analyze subsidence exclusively within the city limits of Ahmedabad.

The average Line of Sight (LOS) velocity (Figure 7) was employed to visually represent the extent and variability of subsidence within the study area. Figure 7 illustrates the mean LOS velocity map spanning from the year 2020 to 2023, providing insights into the spatial distribution of surface displacement across Ahmedabad. The distribution of average LOS land subsidence exhibited a distinct pattern at two different locations within the city i.e. - Southwest and Southeast region of Ahmedabad. Within these regions, the average LOS velocity varied from -1.5 to -3.0 cm/year and -2 to -3.5 cm/year, respectively. Negative LOS velocities denote areas experiencing subsidence, while positive values indicate upliftment. The study identified a noteworthy average subsidence rate in Ahmedabad's urban region. To assess the variation in subsidence rate measurements, the standard deviation of mean LOS velocity was calculated, ranging from 0 to 0.14 cm/year, as depicted in Figure 8. Lower standard deviation values signify greater accuracy in deformation measurement using SBAS InSAR. Three cross-sectional profiles have been drawn over the Southwest and Southeast region (Figure 9). The study carried out by Dumka et al., 2021 based on Persistent Scatterer Interferometry (PSI) technique observed maximum upto 25 mm/year subsidence during 2017 to 2020 in Bopal and Vatva region.

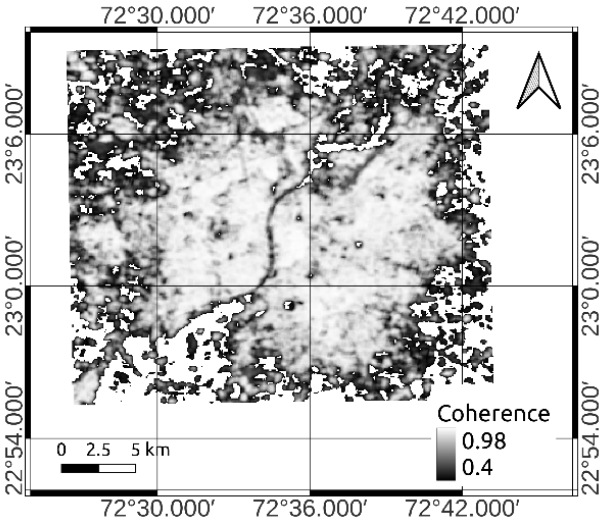

Figure 6. Average coherence map of the Ahmedabad region

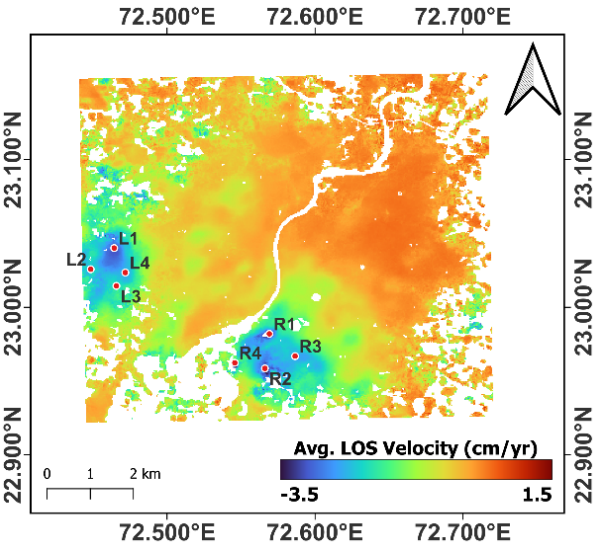

Figure 7. Mean LOS velocity for Ahmedabad derived from SBAS InSAR analysis. Negative values represent subsidence rate

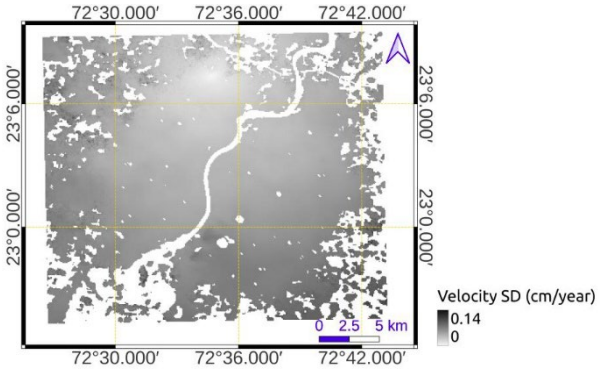

Figure 8. Standard deviation of mean LOS velocity

3.2 Groundwater Level Monitoring Across Distributed Wells

A detailed reports has been published by the CGWB for the Gujarat where records of the long-term well’s water levels was given for the multiple years. Based on the given data, the fluctuation of Ahmedabad district’s well water level of certain months of year 2014, 2016, 2017, 2018, 2019, 2020, 2021 and 2022 were compared with the decadal average water levels for the same months. Particularly, the ground water level record of Ahmedabad district of May (pre-monsoon), August (during-monsoon), November (post-monsoon) of the year 2014, 2016, 2017, 2018, 2019, 2020, 2021, and 2022 and January (post-monsoon) of the year 2015, 2017, 2018, 2019, 2020, 2021, 2022 and 2023 have been compared with the decadal average water level changes during 2004-2013, 2006-2015, 2007-2016, 2008-2017, 2009-2018, 2010-2019, 2011-2020 for May, August, November and 2005-2014, 2007-2016, 2008-2017, 2009-2018, 2010-2019, 2011-2020, 2012-2021 for January, respectively.

Year-wise monthly (May, Aug, Nov and Jan) data of number of wells showing rise and fall in water level at various depths from CGWB for Ahmedabad district were compiled and plotted in the form of graphs (Figure 10).

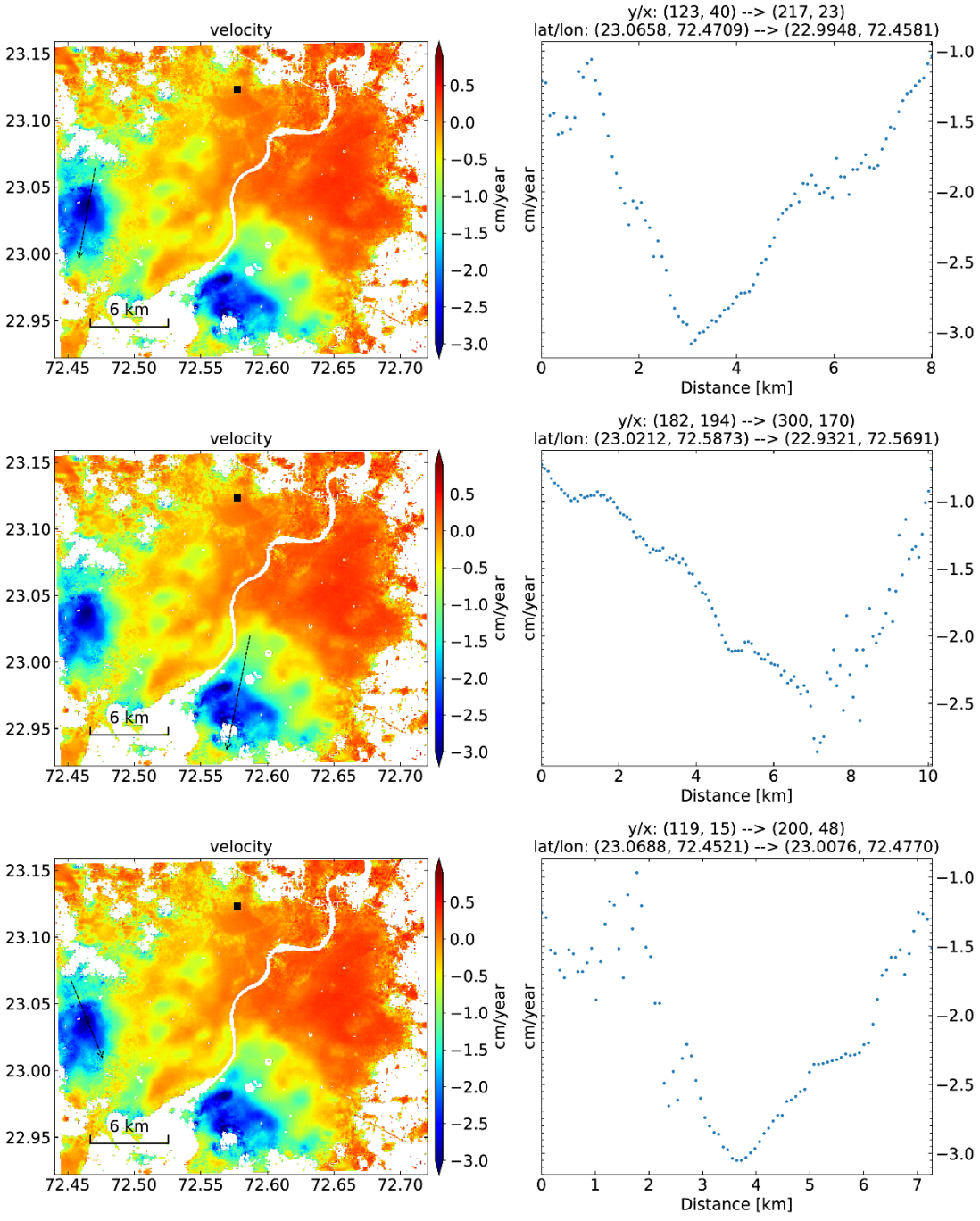

Figure 9. LOS velocity cross-sectional profiles across Southwest and Southeast regions of Ahmedabad

This contribution has been peer-reviewed. The double-blind peer-review was conducted on the basis of the full paper.
https://doi.org/10.5194/isprs-annals-X-G-2025-613-2025 | © Author(s) 2025. CC BY 4.0 License.

Categorically, following observations were derived based on the CGWB data (Figure 10)-

a. General groundwater trends- rising groundwater levels: For most months, except 2016 and 2018, there is a trend of rising groundwater levels at 0-2 m and 2-4 m depths when compared to the decadal average. This indicates an overall positive trend in groundwater levels for most years, suggesting an increase in recharge or reduction in depletion for these periods.
b. Year-specific anomalies- 2016 and 2018 exceptions: The years 2016 and 2018 show a significant number of wells with falling groundwater levels at 0-2 m and 2-4 m depths. These anomalies suggest that these years experienced conditions that led to reduced groundwater levels, which could be due to lower rainfall (refer Figure 2), higher water extraction rates, or other environmental stresses affecting groundwater recharge.
c. Seasonal variations- post-monsoon vs. during-monsoon: Groundwater levels generally rise more during post-monsoon months (November and January) compared to during-monsoon months (August), except for 2016 and 2018. This indicates that groundwater recharge may be more effective or evident after the monsoon period rather than during it, possibly due to the delayed infiltration and accumulation of rainwater. Also, the data shows that the number of wells rising or falling varies from month to month, reflecting seasonal changes in groundwater recharge and extraction patterns.
d. Depth-specific Observations- Shallow vs. Deep Wells: Shallow wells (0-2 m) often show more significant rises or falls compared to deeper wells (2-4 m and >4 m). This may be due to the more immediate influence of seasonal rainfall on shallow wells, while deeper wells may show more gradual changes.
e. Regional disparities- variation across district: The data indicates that the entire Ahmedabad district does not exhibit a uniform trend in groundwater depletion or rise. Some regions may show significant improvements or declines in groundwater levels, highlighting variability across the district.
f. Specific region- notable groundwater rise in Bopal: The Bopal region, in particular, recorded a rise in groundwater levels- 32.87 m, 22.26 m, and 24.89 m in May, Aug and November 2021, respectively with respect to decadal average. This indicates that Bopal experienced a substantial recharge or improvement in groundwater conditions in year 2021 compared to other regions of Ahmedabad district. Also, at district-level, more rainfall (above 600 mm) has been observed during year 2019 and 2020, which may lead to rise in ground water condition at local scale in the subsequent year 2021.
g. According to data from the CGWB, the groundwater level in the Bopal area (Southwest region of Ahmedabad) significantly decreased from around 11 meters in near mid of 2005 to less than 2 meters by 2019 (as cited by Dumka et al., 2021). Similarly, in the Vatva area (Southeast region of Ahmedabad), the water level dropped from approximately 42 meters in 2005 to about 28 meters in 2019 (as reported by Dumka et al., 2021). A study conducted by Dumka et al. 2021 based on PSI technique correlated observed land subsidence (maximum upto 25 mm/year) during period 2017 to 2020 in both the regions i.e. Bopal and Vatva with groundwater water level depletion. It's important to note that the declining groundwater trend observed in the Bopal and Vatva regions from year 2005 to 2019, as shown in Dumka et al. (2021) based on CGWB non-uniform (not collected in fixed temporal interval) time-series data, actually reflects water levels, which usually varies during different months (or seasons) in a year. Generally, the groundwater levels vary across seasons due to climatic conditions (Vitola et al. 2013), agricultural water requirement (Ha et al. 2021) and human factors (Zaveri et al. 2016). For instance, water levels tend to rise after the rainy season (also seen in Figure 10) when rainfall increases recharge, while in dry seasons, less rainfall, more ground water consumption and higher evaporation rates cause levels to drop. Moreover, the demand for groundwater intensifies during the growing season, as agricultural irrigation increases, further contributing to the decline in water levels. Therefore, month to month comparison of ground water level on yearly basis as illustrated in Figure 10, would provide us true understanding of ground water depletion/recovery. Furthermore, for the later duration i.e. year 2020 to 2023, current study found maximum subsidence upto 35 mm/year derived through SBAS InSAR technique in the Bopal and the Vatva regions.
h. At the district level (for Ahmedabad district), a significant number of wells exhibited rise in groundwater levels from 2014 to 2022 compared to the decadal average, indicating an overall positive trend in groundwater availability (Figure 10). This improvement is evident despite the exceptions in 2016 and 2018, where groundwater levels fall in as many or more wells than those showing an increase in water levels. Overall, across the monitored wells, there hasn't been a consistent or widespread decline in water levels over time. In other words, while some wells may have experienced drops in water levels, this trend has not been universal or continuous across a significant number of wells. There may be periods of stability, recovery, or variability in the water levels of many wells rather than a uniform decrease.

3.3. Ground water utilization for Agriculture

Both crops, rice as well as wheat showed gradual increases in production between 1995-96 and 2021-22, reflecting overall agricultural growth (Figure 3a) in Ahmedabad district. However, around 2010-2011, a significant divergence occurs, with wheat production experiencing a sharp increase that allows it to surpass rice production. Post-2010, wheat consistently outproduces rice, with particularly high production levels peaking around 2018-2019. This period marks the dominance of wheat. The sharp increase in irrigated land around 2010-2011 (Figure 3b) corresponds with a similar rise in wheat production, as seen in Figure 3a, indicating that irrigation was a key factor in boosting yields. The consistent dominance of irrigated land over unirrigated land throughout the period underscores the dependency of wheat production on reliable water sources, potentially ground water. Furthermore, over the years, irrigated wheat production has shown a steady increase, with notable spikes around 2010-11 and 2019-20 (Figure 3c). In contrast, unirrigated wheat production has remained relatively stable, with little variation throughout the period. This stability indicates that unirrigated regions have not experienced significant advancements, remaining reliant on natural rainfall. Importantly, it seems increase in crop production in the region has not causes ground water depletion.

4. CONCLUSION

Significant land subsidence was detected in the Ahmedabad urban area from 2020 to 2023 using the Sentinel-1 InSAR technique. The subsidence aligns with observed groundwater levels in specific regions (Bopal and Vatva), which have shown a declining trend between 2005 and 2019. Typically, land

subsidence lags behind groundwater depletion, causing subsidence even when groundwater levels begin to recover. At the district level, many wells showed an increase in groundwater levels from 2014 to 2022 (except in 2016 and 2018), indicating an overall positive trend in groundwater availability. Thus, the observed subsidence can be linked to localized groundwater over-extraction and the area’s specific hydrogeological conditions, which may differ from regional trends.

Acknowledgement

We sincerely acknowledge the European Space Agency (ESA) for providing Sentinel-1 time-series InSAR data and the Central Ground Water Board (CGWB), India, for making long-term well water level records available for Gujarat. We also extend our gratitude to the Alaska Satellite Facility (ASF) for providing the computational resources and platforms used for Sentinel-1 InSAR data processing and analysis.

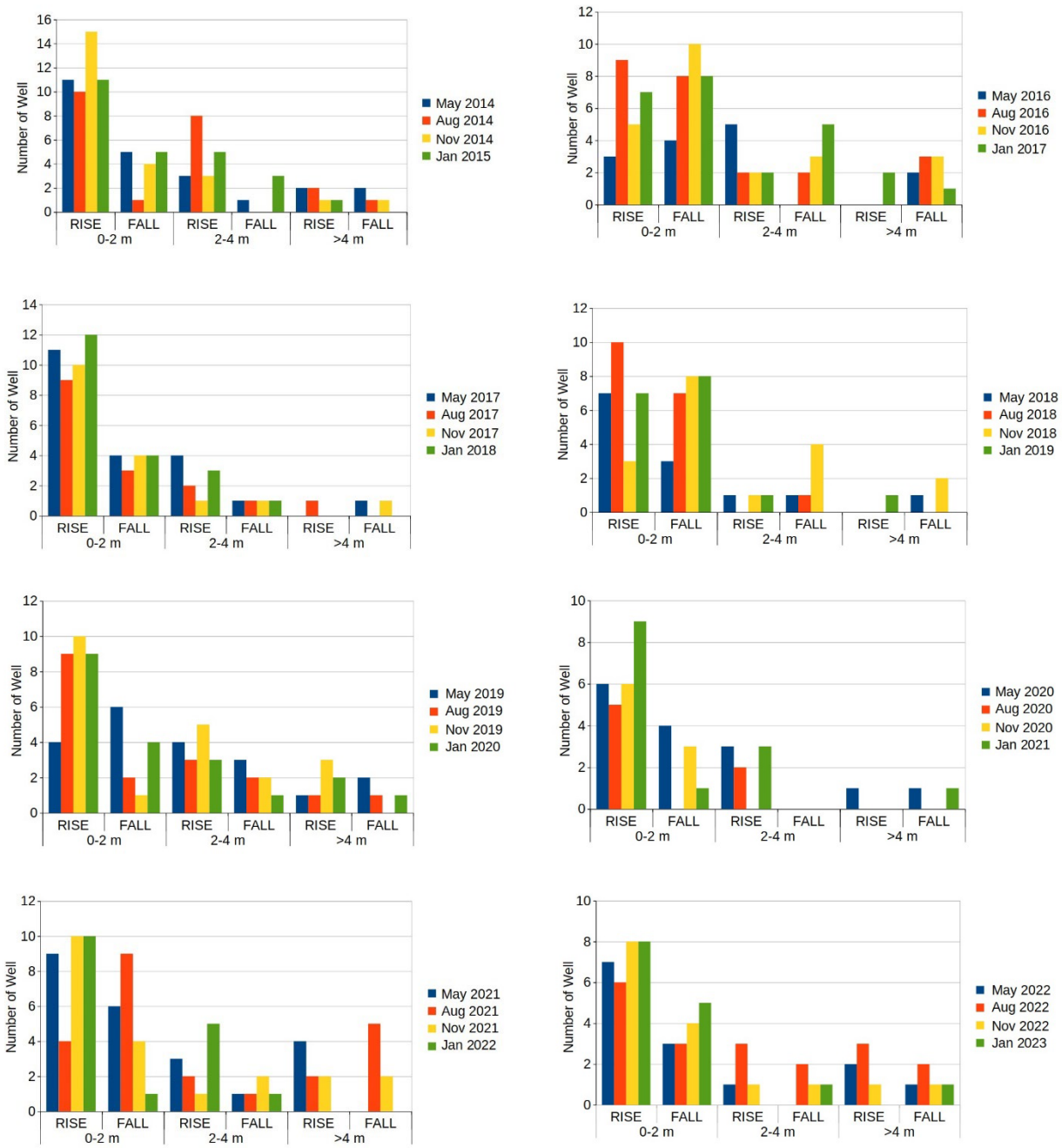

Figure 10. Year-wise monthly (May, Aug, Nov and Jan) data of number of wells showing rise and fall in water level at various depths (0-2 m, 2-4 m and >4 m)

https://doi.org/10.5194/isprs-annals-X-G-2025-613-2025

References

Abidin, H. Z., Andreas, H., Djaja, R., Darmawan, D., & Gamal, M. (2008). Land subsidence characteristics of Jakarta between 1997 and 2005, as estimated using GPS surveys. Gps Solutions, 12, 23-32

Albano, M., Chiaradonna, A., Saroli, M., Moro, M., Pepe, A., & Solaro, G. (2024). InSAR Analysis of Post-Liquefaction Consolidation Subsidence after 2012 Emilia Earthquake Sequence (Italy). Remote Sensing, 16(13), 2364.

Alipour, S., Motgah, M., Sharifi, M. A., & Walter, T. R. (2008, November). InSAR time series investigation of land subsidence due to groundwater overexploitation in Tehran, Iran. In 2008 Second Workshop on Use of Remote Sensing Techniques for Monitoring Volcanoes and Seismogenic Areas (pp. 1-5). IEEE.

Aobpaet, A., Cuenca, M. C., Hooper, A., & Trisirisatayawong, I. (2013). InSAR time-series analysis of land subsidence in Bangkok, Thailand. International Journal of Remote Sensing, 34(8), 2969-2982.

Central Ground Water Board (2023). National Compilation on Dynamic ground water resources of India. https://cgwb.gov.in/cgwbpnm/public/uploads/documents/17014272111704550895file.pdf

Ministry of Water Resources, River Development and Ganga Rejuvenation, Annual Report 2013-14. http://wrmin.nic.in/writereaddata/AR_2013-14.pdf.

Chaussard, E., Wdowinski, S., Cabral-Cano, E., & Amelung, F. (2014). Land subsidence in central Mexico detected by ALOS InSAR time-series. Remote sensing of environment, 140, 94-106.

Chen, G., Zhang, Y., Zeng, R., Yang, Z., Chen, X., Zhao, F., & Meng, X. (2018). Detection of land subsidence associated with land creation and rapid urbanization in the chinese loess plateau using time series insar: A case study of Lanzhou new district. Remote Sensing, 10(2), 270.

Chen, Y., Zhang, G., Ding, X., & Li, Z. (2000). Monitoring earth surface deformations with InSAR technology: principles and some critical issues. Journal of Geospatial Engineering, 2(1), 3-22.

Choudhury, P., Gahalaut, K., Dumka, R., Gahalaut, V. K., Singh, A. K., & Kumar, S. (2018). GPS measurement of land subsidence in Gandhinagar, Gujarat (Western India), due to groundwater depletion. Environmental Earth Sciences, 77, 1-5.

Cigna, F., & Tapete, D. (2021). Satellite InSAR survey of structurally-controlled land subsidence due to groundwater exploitation in the Aguascalientes Valley, Mexico. Remote Sensing of Environment, 254, 112254.

Cigna, F., & Tapete, D. (2022). Urban growth and land subsidence: Multi-decadal investigation using human settlement data and satellite InSAR in Morelia, Mexico. Science of The Total Environment, 811, 152211.

Dehghani, M., Valadan Zoej, M. J., Entezam, I., Mansourian, A., & Saatchi, S. (2009). InSAR monitoring of progressive land subsidence in Neyshabour, northeast Iran. Geophysical Journal International, 178(1), 47-56.

Dong, S., Samsonov, S., Yin, H., Ye, S., & Cao, Y. (2014). Time-series analysis of subsidence associated with rapid urbanization in Shanghai, China measured with SBAS InSAR method. Environmental earth sciences, 72, 677-691.

Fatholahi, N., Akhoondzadeh Hanzaei, M., & Bahroudi, A. (2018). Study of land subsidence due to the oil extraction using Radar Interferometry (InSAR). Scientific-Research Quarterly of Geographical Data (SEPEHR), 27(105), 23-34.

Ferretti, A., Colombo, D., Fumagalli, A., Novali, F., & Rucci, A. (2015). InSAR data for monitoring land subsidence: time to think big. Proceedings of the International Association of Hydrological Sciences, 372(372), 331-334.

Gabriel, A. K., Goldstein, R. M., & Zebker, H. A. (1989). Mapping small elevation changes over large areas: Differential radar interferometry. Journal of Geophysical Research: Solid Earth, 94(B7), 9183-9191.

Garg, S., Motagh, M., Indu, J., & Karanam, V. (2022). Tracking hidden crisis in India’s capital from space: implications of unsustainable groundwater use. Scientific reports, 12(1), 651.

Ghorbani, Z., Khosravi, A., Maghsoudi, Y., Mojtahedi, F. F., Javadnia, E., & Nazari, A. (2022). Use of InSAR data for measuring land subsidence induced by groundwater withdrawal and climate change in Ardabil Plain, Iran. Scientific Reports, 12(1), 13998.

Gorelick, N., Hancher, M., Dixon, M., Ilyushchenko, S., Thau, D., & Moore, R. (2017). Google Earth Engine: Planetary-scale geospatial analysis for everyone. Remote sensing of Environment, 202, 18-27.

Ha, K., Lee, E., An, H., Kim, S., Park, C., Kim, G. B., & Ko, K. S. (2021). Evaluation of seasonal groundwater quality changes associated with groundwater pumping and level fluctuations in an agricultural area, Korea. Water, 13(1), 51.

Hejmanowski, R., Malinowska, A. A., Witkowski, W. T., & Guzy, A. (2019). An analysis applying InSAR of subsidence caused by nearby mining-induced earthquakes. Geosciences, 9(12), 490.

Hu, B., Chen, J., & Zhang, X. (2019). Monitoring the land subsidence area in a coastal urban area with InSAR and GNSS. Sensors, 19(14), 3181.

Ikehara, M. E. (1994). Global Positioning System surveying to monitor land subsidence in Sacramento Valley, California, USA. Hydrological Sciences Journal, 39(5), 417-429.

Kadiyan, N., Chatterjee, R. S., Pranjal, P., Agrawal, P., Jain, S. K., Angurala, M. L., ... & Champati Ray, P. K. (2021). Assessment of groundwater depletion–induced land subsidence and characterisation of damaging cracks on houses: A case study in Mohali-Chandigarh area, India. Bulletin of Engineering Geology and the Environment, 80, 3217-3231.

Kumar, H., Syed, T. H., Amelung, F., Agrawal, R., & Venkatesh, A. S. (2022). Space-time evolution of land subsidence in the National Capital Region of India using ALOS-1 and Sentinel-1 SAR data: Evidence for groundwater overexploitation. Journal of Hydrology, 605, 127329.

Sahu, P., & Sikdar, P. K. (2011). Threat of land subsidence in and around Kolkata city and East Kolkata Wetlands, West Bengal, India. Journal of earth system science, 120, 435-446.

Shankar, H., Singh, D., & Chauhan, P. (2024). Investigation of groundwater induced land subsidence in Ludhiana City using InSAR and Sentinel-1 data. Quaternary Science Advances, 13, 100151.

Sharif, A., Omar, K., & Kadir, M. (1997, September). Modelling of Land Subsidence Induced By Ground Water Withdrawal Using GPS. In Proceedings of the 10th International Technical Meeting of the Satellite Division of The Institute of Navigation (ION GPS 1997) (pp. 1207-1215).

Sneed, M., & Brandt, J. T. (2007). Detection and measurement of land subsidence using global positioning system surveying and interferometric synthetic aperture radar, Coachella Valley, California, 1996-2005 (No. 2007-5251). Geological Survey (US).

Suhag, R. (2016). Overview of ground water in India. PRS On Standing Committee On Water Resources, Legislative Research, (February), 12p.

Torres, R., Snoeij, P., Geudtner, D., Bibby, D., Davidson, M., Attema, E., ... & Rostan, F. (2012). GMES Sentinel-1 mission. Remote sensing of environment, 120, 9-24.

Vitola, I., Vircavs, V., Abramenko, K., Lauva, D., & Veinbergs, A. (2013). Precipitation and air temperature impact on seasonal variations of groundwater levels. Environmental and Climate Technologies, 10(2012), 25-33.

Zakaria, Z. A., Ebadi, H., & Ahmadi, F. F. (2023). The feasibility of using InSAR technique to measure land subsidence caused by petroleum extraction. Journal of Petroleum Geomechanics; Vol, 6(1).

Zaveri, E., Grogan, D. S., Fisher-Vanden, K., Frolking, S., Lammers, R. B., Wrenn, D. H., ... & Nicholas, R. E. (2016). Invisible water, visible impact: groundwater use and Indian agriculture under climate change. Environmental Research Letters, 11(8), 084005.